Journal of Power Sources 218 (2012) 73–78

Contents lists available at SciVerse ScienceDirect

Journal of Power Sources

journal homepage: www.elsevier.com/locate/jpowsour

Electrocatalytic performance of environmentally friendly synthesized gold nanoparticles towards the borohydride electro-oxidation reaction

Luiz H.S. Gasparotto*, Amanda C. Garcia, Janaina F. Gomes, Germano Tremiliosi-Filho

Instituto de Química de São Carlos, Universidade de São Paulo, 13560-970 São Carlos, São Paulo, Brazil

HIGHLIGHTS

- Environmentally friendly synthesis of Au nanoparticles.
- Production of Au nanoparticles directly onto carbon using glycerol as reducing agent in alkaline medium.
- High activity of Au nanoparticles towards the borohydride oxidation in comparison to bulk Au.

GRAPHICAL ABSTRACT

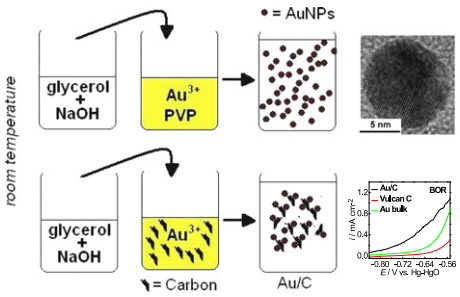

ARTICLE INFO

Article history:
Received 23 April 2012
Received in revised form
15 June 2012
Accepted 18 June 2012
Available online 23 June 2012

Keywords:
Gold nanoparticles
Glycerol
Alkaline medium
Borohydride

ABSTRACT

In this paper we report a simple and environmentally friendly synthesis of gold nanoparticles (AuNps) and their electrocatalytic activity for borohydride oxidation reaction (BOR). Ultraviolet spectroscopy (UV–vis) and transmission electron microscopy (TEM) confirmed the formation of poly(vinyl pyrrolidone)-protected colloidal AuNps through direct reduction of Au^{3+} by glycerol in alkaline medium at room temperature. For the BOR tests the AuNps were directly produced onto carbon to yield the Au/C catalyst. Levich plots revealed that the process occured via 7.2 electrons, therefore near the theoretical value of 8 electrons. When compared to bulk Au, the gold nanoparticles presented enhanced catalytic properties since the onset potential for BOR was shifted 200 mV towards negative potentials.

1. Introduction

Noble metal nanoparticles have been the target of growing interest due to their physicochemical properties which are significantly distinct from their bulk counterparts [1]. As an example, gold is known to be shiny, yellow, non-tarnishing and non-magnetic. In contrast, nanosized Au particles appear red to the naked eye, their properties are less noble than those of the bulk solid variant, present excellent catalytic properties [2] and considerable magnetism [3]. Particularly, metallic nanoparticles have been extensively employed as electrocatalysts for fuel cell applications [4,5]. Among various fuel cells, the direct borohydride fuel cell (DBFC) [6–8] has instigated the interest of many scientists due to the chemical stability and non-flammable nature of the solid fuel ($NaBH_4$), a high cell voltage (1.64 V) and the good specific capacity (5.7 Ah g^{-1}, higher than that of methanol) [9]. It is known that the performance of the DBFC is strongly dependent on both electrode material and borohydride concentration. Despite Chatenet et al. [10] not considering gold as a faradaic-efficient electrocatalyst for the borohydride oxidation reaction (BOR), numerous works [11–14] obtained high coulombic efficiency with Au electrocatalyst, which is attributed to its low activity towards hydrolysis

* Corresponding author. Tel.: +55 16 3373 9934.
E-mail address: lhgasparotto@iqsc.usp.br (L.H.S. Gasparotto).

0378-7753/$ – see front matter © 2012 Elsevier B.V. All rights reserved.
http://dx.doi.org/10.1016/j.jpowsour.2012.06.064

of the BH_4^- anion. The hydrolysis or electro-oxidation of BH_4^- require the break of the B–H, which is fast on Pt(111) and slow on Au(111) [15,16].

The polyol [17–19] and microwave-assisted [20–24] methods have been extensively employed in the preparation of noble nanoparticles. The polyol method typically consists in refluxing a mixture of a precursor salt (e.g. $AuCl_3$ or $AgNO_3$), a stabilizing agent [e.g. poly (vinyl pyrrolidone) (PVP)] and a polyalcohol (e.g. ethylene glycol) at ~160–240 °C for 2–12 h, which is tedious, time and energy consuming. The microwave-assisted approach also requires high temperature and has the further inconvenient of demanding a microwave generator. Another popular reducing agent is hydrazine [25–27]. Although hydrazine is quite efficient as a reducing agent it should be avoided because it has many drawbacks: it is carcinogenic, extremely dangerous towards health and environment and very unstable [28] (specially in its anhydrous form). In this work we employed an eco-friendly route to produce gold nanoparticles (AuNps) based on reduction of Au^{3+} by glycerol in alkaline medium at room temperature. The AuNps can be obtained as a colloidal dispersion as well as directly anchored in carbon (Au/C), with the latter allowing the direct application for the BOR. The carbon-supported Au nanoparticles displayed an excellent performance towards the BOR by decreasing the onset potential for BH_4^- oxidation when compared to the bulk Au. Furthermore, compared to above-mentioned methods, glycerol is a greener option since it is non-toxic and readily biodegradable under aerobic conditions.

2. Experimental

2.1. Reactants and instrumentation

All chemicals used in this work were of analytical grade and used without further purification. UV–vis spectra of the AuNps colloidal suspension were acquired with a Varian/Cary 5G spectrophotometer. For the TEM experiments, cooper coated grids were immersed into the AuNps colloidal and Au/C suspensions and allowed to dry overnight in a desiccator. The grids were then analyzed using either a TEM FEI Tecnai with an accelerating potential of 200 kV or a Magellan XRH scanning electron microscope in the transmission mode with an accelerating potential of 30 kV. X-ray diffraction (XRD) measurements were carried out using a Rigaku diffractometer. Energy-dispersive X-ray spectroscopy (EDX) was conducted on a Zeiss-Leica/440 to determine the composition of the Au/C catalyst. Electrochemical experiments were conducted with an AUTOLAB 30 potentiostat/galvanostat controlled by the GPES software.

2.2. Synthesis of colloidal and carbon-supported AuNps

In a typical experiment for colloidal AuNps production, known amounts of PVP (Aldrich, MW = 10,000) and $AuCl_3$ (30% wt in HCl, Aldrich) were dissolved in 5 ml of ultrapure water. In a separate flask, determined quantities of glycerol (Aldrich) and NaOH (Aldrich) were dissolved in 5 ml of ultrapure water. The glycerol–NaOH solution was then added to the $AuCl_3$-PVP solution to yield the following final concentrations: 0.5 mmol L^{-1} Au^{3+}, 0.1 mol L^{-1} NaOH and 10 g L^{-1} PVP. The glycerol concentration was varied from 0.66 mmol L^{-1} to 3.0 mol L^{-1} and all the other parameters were kept constant. The initial pale yellow mixture immediately turned into a deep red characteristic of colloidal AuNps. The colloidal suspensions were then characterized with UV–vis and TEM. For the BOR experiments the AuNps were produced directly onto Vulcan carbon (Au/C) without stabilization by PVP. In this way a potential influence of PVP on BOR was eliminated. The synthesis of the Au/C catalyst consisted in sonicating an appropriate amount of XC-72 Vulcan carbon in a known volume of ultrapure water and then adding a fixed amount of $AuCl_3$ under stirring to promote homogenization. Afterwards, another aqueous solution containing glycerol and NaOH was added to give the following concentrations: 0.50 mmol L^{-1} $AuCl_3$, 1.0 mol L^{-1} glycerol and 0.10 mol L^{-1} NaOH. The black suspension was kept during 24 h under stirring at room temperature and then washed, filtered and dried at 80 °C for 12 h. The Au/C electrocatalyst was characterized with EDX to determine the Au/C load and by XRD to observe the diffraction pattern. The average crystallite size was estimated using Scherrer equation [29]:

$$D = k\lambda/B\cos\theta \quad (1)$$

where D is the average crystallite size in Å, k is a coefficient taken here as 0.9, λ is the wavelength of the X-rays used (1.5406 Å), B is the width of the diffraction peak at half height in radians, and θ is the angle at the position of the peak maximum.

2.3. Electrochemical measurements

The electrochemical experiments were conducted in a three-electrode conventional cell. A glassy-carbon rotating-disk (RDE), a gold foil and an Hg–HgO in 1.0 mol L^{-1} NaOH (−0.926 V *vs.* reversible hydrogen electrode) were employed as working, counter and reference electrodes, respectively. A glassy carbon disk ($\varphi = 5$ mm, geometric area = 0.196 cm^2) was used as substrate to prepare active layers of Au/C. For the preparation of the catalytic layer 2.0 mg of the Au/C powder was suspended in a mixture containing 1 mL of isopropyl alcohol and 20 μL of a Nafion solution (5 wt % in low aliphatic alcohol, from DuPont). After ultrasonic homogenization, 20 μL of this ink was deposited onto the glassy carbon electrode and the solvent was then evaporated at room temperature. Rotating-disk electrode measurements were performed in O_2-free 1.0 mol L^{-1} NaOH + 1.0 mmol L^{-1} $NaBH_4$ solutions prepared with ultrapure water.

3. Results and discussion

3.1. Chemical and physical characterizations of the colloidal and carbon-supported AuNps

The use of PVP was found to be imperative to obtain stable colloidal AuNps. In the absence of PVP, the gold nanoparticles tended to agglomerate and precipitate in the bottom of the reaction vessel. This means that glycerol itself is not capable of concomitantly functioning as reducing and stabilizing agent. Fig. 1A shows a collection of the UV–vis spectra of the colloidal AuNps prepared at room temperature (~25 °C) using glycerol at different concentrations in alkaline medium and PVP as stabilizing agent. The absorbance increased with increasing glycerol concentration. The colloidal AuNps spectra had a maximum absorbance at around 520 nm regardless of the glycerol concentration, a value which agrees very well with data in literature [1,30,31]. The red color is due to the surface plasmon band (SPB), a broad absorption band in the visible region. The SPB reflects the collective oscillations of the electron gas (electrons of the conduction band) at the surface of nanoparticles. The SPB provides a quick assessment about the size regime of some metal particles (e.g. Ag and Au). The fact that the SPB position did not vary with the glycerol concentration implies that the size and distribution of the AuNps are roughly the same [32] independently of the glycerol concentration. Furthermore, an SPB located at around 520 nm has been correlated with spherical particles of 22 nm [32], 15 nm [1] and 7.9 nm [30] in size. The SPB

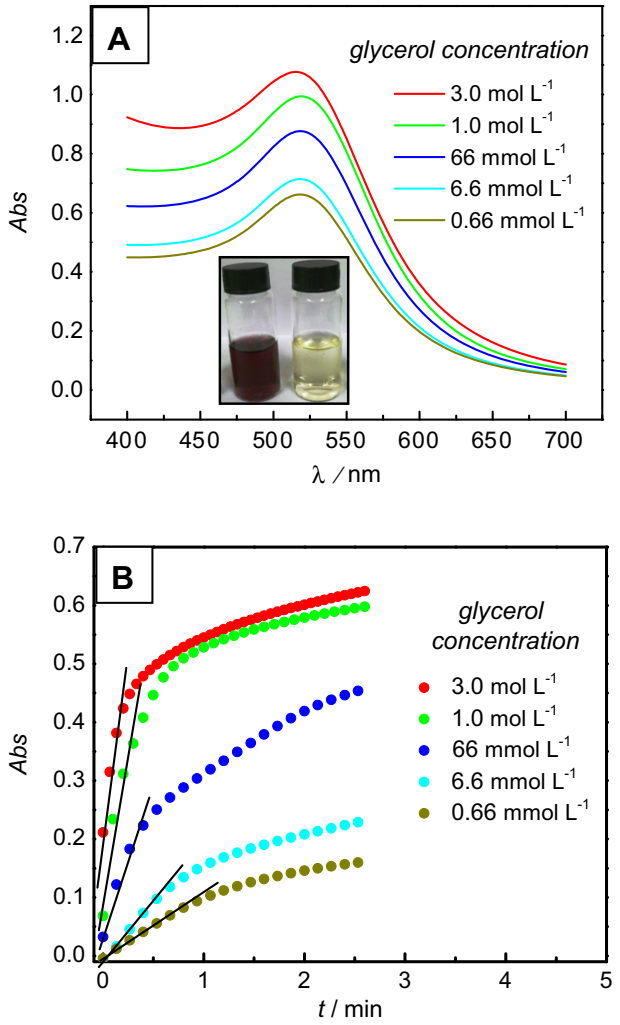

Fig. 1. (A) TEM image of the colloidal AuNps and (B) high-resolution TEM of a single nanoparticle. Condition of synthesis: 0.10 mol L^{-1} glycerol, 0.10 mol L^{-1} NaOH, 10 g L^{-1} PVP and 0.50 mmol L^{-1} $AuCl_3$. θ = 25 °C.

maximum is also influenced by the particle form, medium dielectric constant and temperature, which may account for the reported differences in size. Moreover, the refractive index of the solvent also induces a shift of the SPB [33]. Therefore, in our case, we can only infer that the mean particle size is roughly the same for the different glycerol concentrations, but a direct correlation with a specific size is not possible (given that the above-referenced works employed distinct experimental conditions). The *inset* of Fig. 1A shows that a red-colored solution is obtained only in alkaline media. Some authors have suggested that polyols dehydrate to aldehydes, which, in turn, reduce metallic ions to elemental metal. In our opinion the aldehyde is not responsible for the reduction. We also tried to synthesize AuNps by employing acetaldehyde as reducing agent in both acid and neutral medium and no nanoparticle formation was observed. Therefore the aldehyde is not the responsible for the reduction. At high pH the alcohol is deprotonated and the generated anion may be responsible for the reduction. Another important question is how the glycerol concentration affects the rate of the reaction. Fig. 1B depicts the effect of the glycerol concentration on the velocity of AuNps formation. The experiments were carried out by fixing the wavelength of 520 nm and measuring the absorbance variation immediately after mixing the reactants directly in the UV cuvette. In general, the rate of nanoparticle formation rose with increasing glycerol concentration as shown by the slopes of the lines taken in the beginning of the experiments. It is noteworthy that no significant absorbance increment was observed when the glycerol concentration was increased from 1.0 mol L^{-1} and 3.0 mol L^{-1}. Furthermore, the maximum velocity can already be obtained with the concentration of 1.0 mol L^{-1}. Note that the initial rates of nanoparticle formation (the slopes of the straight lines of Fig. 1B) increased up to the glycerol concentration of 1.0 mol L^{-1}.

Analysis of TEM images of AuNps obtained at an intermediate glycerol concentration of 0.10 mol L^{-1} (Fig. 2A) indicated that most of nanoparticles obtained from the process were spherical in shape and around 10 nm in size. High-resolution TEM in Fig. 2B showed that the AuNps are quite defective (some defects are indicated by red arrows) and polycrystalline. It is important to emphasize that in the present work we did not pursue the synthesis optimization (in order to obtain monodispersivity, for example), which could be achieved by studying the influence of parameters such as temperature, nature and concentration of the stabilizer, concentration of the precursor, pH etc. We rather report a successful and straightforward way of producing gold nanoparticles at room temperature with an abundant and environmentally friendly reducing agent.

The production of the Au/C for BOR was conducted at a glycerol concentration of 1.0 mol L^{-1} since no concentration higher than 1.0 mol L^{-1} is necessary to attain the maximum formation rate of AuNps, as shown in Fig. 1B. As discussed in the experimental section, the AuNps for BOR were produced directly on carbon

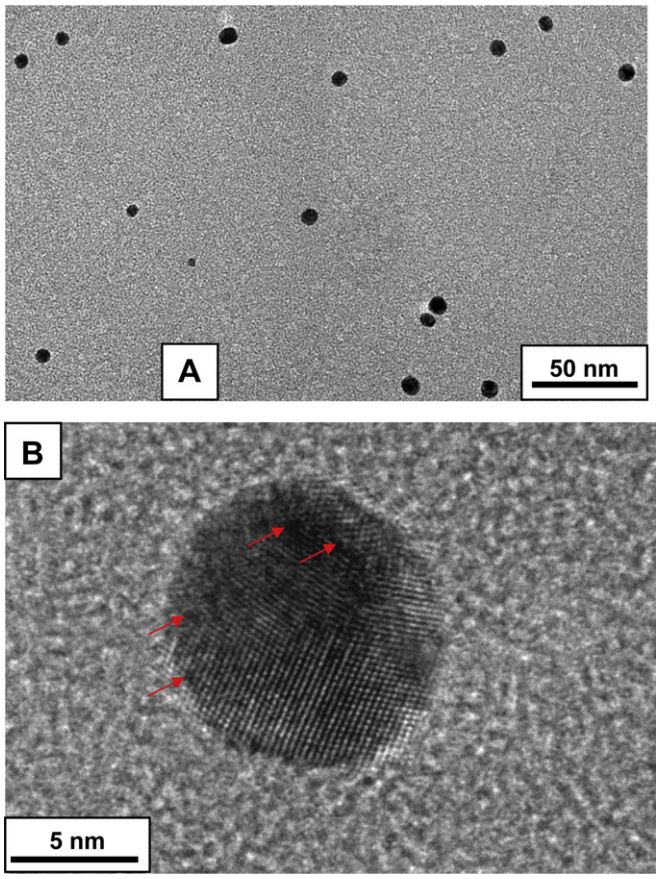

Fig. 2. (A) TEM images of the colloidal AuNps and (B) high-resolution TEM of a single nanoparticle. Condition of synthesis: 0.10 mol L^{-1} glycerol, 0.10 mol L^{-1} NaOH, 10 g L^{-1} PVP and 0.50 mmol L^{-1} $AuCl_3$ at 25 °C.

without stabilization by PVP. The goal was to avoid any influence of PVP on BOR, however a complete control of the synthesis is expected to be lost. The XRD pattern of the Au/C (Fig. 3) revealed the typical face centered cubic (fcc) structure of gold and was further analyzed using the Scherrer equation in order to estimate the average crystallite size. The mean crystallite size estimated for the Au/C catalyst resulted in 22 nm. Typical TEM image of the Au/C catalyst acquired with a high angle annular dark field (HAADF) detector is shown in Fig. 4. In this acquisition mode the bright spots are the gold nanoparticles. As expected, the influence of PVP on BOR is eliminated at the cost of the control over the nanoparticle size. One can identify particles from 6 nm to 14 nm. Nevertheless, the Au/C was active towards BOR, as presented in the next section. EDX analyses gave 10% wt of Au onto carbon, therefore we conclude that, based on the initial $AuCl_3$ used in the synthesis, the conversion of gold ions into metal was quantitative.

3.2. Activity of the gold nanoparticles towards the BOR

RDE voltammograms at various rotation rates in deaerated 1.0 mol L^{-1} NaOH + 1.0 mmol L^{-1} $NaBH_4$ were conducted between −0.88 V and 0.3 V *vs.* Hg–HgO and the results are displayed in Fig. 5A. In all cases the currents were normalized by the geometric area of the electrode. The onset for BH_4^- oxidation is about −0.65 V, implying an overpotential of 0.69 V since the theoretical oxidation potential of BH_4^- is −1.34 V *vs.* Hg–HgO. Mass-transport limited current region is evident from −0.4 V to 0.3 V. Although the RDE voltammograms exhibit a somewhat poorly defined kinetic region, an expansion of it (*inset* of Fig. 5A) shows that the curves do not cross each other. This suggests that, in principle, at sufficiently negative potentials the Au/C did not significantly contributed to the BH_4^- hydrolysis reaction [34], therefore suppressing the hydrogen oxidation reaction (HOR) that could contribute to the kinetic current in that potential region. This is extremely important for fuel cell applications since the inhibition of the BH_4^- hydrolysis would enhance the faradaic efficiency of the electrocatalyst. Depending on the electrode material (for example Au and Pt) and composition of the solution, the eight electrons involved in the BOR may compete with the quasi-spontaneous hydrolysis of BH_4^- (Eq. (2)), either homogeneous in the solution, or heterogeneous at the electrode [35].

$$BH_4^- + xOH^- \rightarrow BO_2^- + (x-2)H_2O + (4-0.5x)H_2 + xe^- \qquad (2)$$

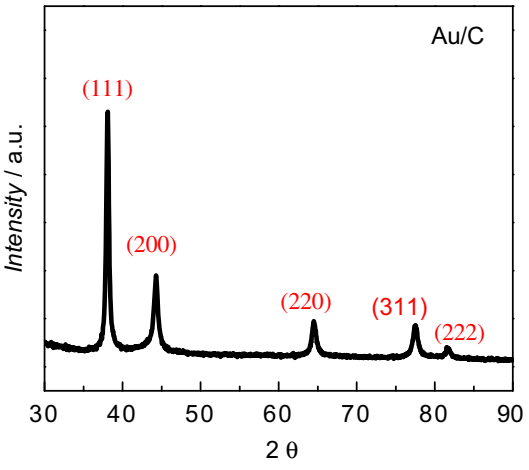

Fig. 3. X-ray diffraction (XRD) pattern of the Au/C. Condition of synthesis: 1.0 mol L^{-1} glycerol, 0.10 mol L^{-1} NaOH, 10 g L^{-1} PVP and 0.50 mmol L^{-1} $AuCl_3$ at 25 °C.

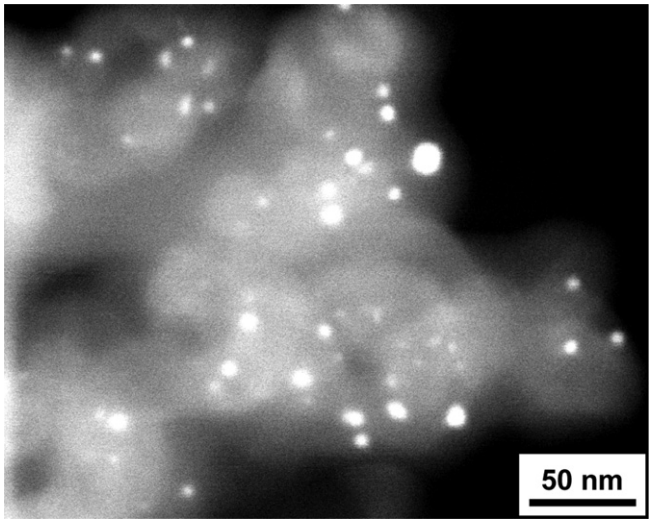

Fig. 4. TEM image acquired with a high angle annular dark field (HAADF) detector. The bright spots are the gold nanoparticles. Condition of synthesis: 1.0 mol L^{-1} glycerol, 0.10 mol L^{-1} NaOH, 10 g L^{-1} PVP and 0.50 mmol L^{-1} $AuCl_3$ at 25 °C.

The occurrence of this latter reaction actually lowers the practical number of electrons exchanged per BH_4^- anion because it generates H_2 at a rather uncontrolled rate, some of which can evolve away from the electrode without being oxidized. As a result, the overall faradaic efficiency electrocatalyst decreases [36]. Fig. 5B shows the corresponding Levich plot at 0.1 V *vs.* Hg–HgO from which the apparent number of electrons involved in the BOR electro-oxidation was estimated to be 7.2. This is in good agreement

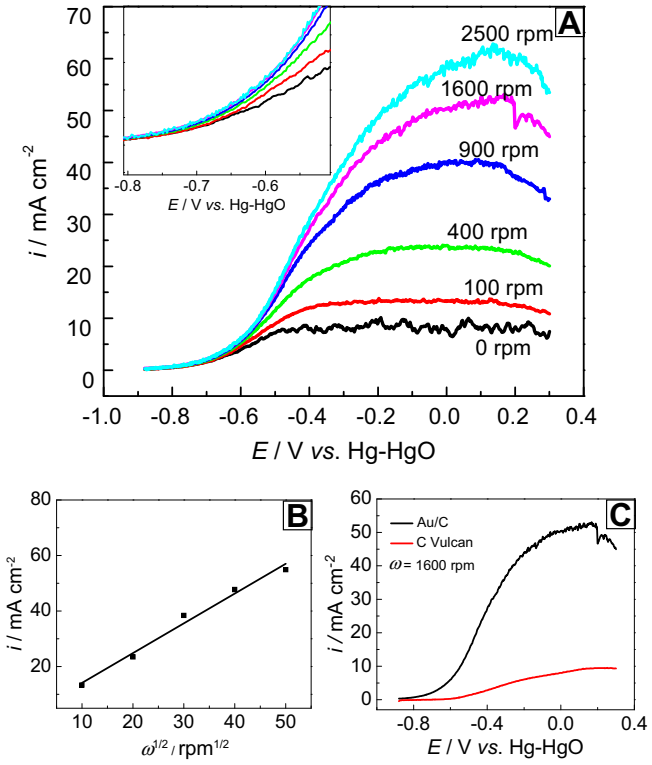

Fig. 5. (A) Steady-state polarization curves for the BOR on Au/C catalyst in deaerated 1.0 mol L^{-1} NaOH + 1.0 mmol L^{-1} $NaBH_4$ at 25 °C. (B) Levich plot at 0.1 V *vs.* Hg–HgO. (C) Steady-state polarization curves for Au/C and Vulcan Carbon at 1600 rpm. Solution: deaerated 1.0 mol L^{-1} NaOH + 1.0 mmol L^{-1} $NaBH_4$ at 25 °C.

with the number of electrons (>7e$^-$) reported in the literature for gold [35,37,38]. In comparison to other metals, lower onset potentials for Pt [35] and Pd [39] were found with the total number of electrons exchanged of four and six, respectively. Finkelstein et al. [40] performed a detailed study on BH_4^- electro-oxidation at Au and Pt and concluded that the reaction mechanism is quite complex. It was found that higher open-circuit voltages can be achieved with Pt than with Au. However, the authors commented that Au anodes are expected to provide higher current at lower voltages.

Another important question is whether the carbon support has an impact on the BOR. Fig. 5C compares the BOR behavior on Vulcan carbon and on the Au/C in deaerated 1.0 mol L^{-1} NaOH + 1.0 mmol L^{-1} $NaBH_4$ at 1600 rpm. It is unarguable that the Au nanoparticles promoted a drastic improvement of the BOR electrocatalysis in terms of both current level and potential onset, however the effect of the carbon support can not be neglected. Fig. 6 presents RDE voltammograms for pure Vulcan carbon at various rotation rates in deaerated 1.0 mol L^{-1} NaOH + 1.0 mmol L^{-1} $NaBH_4$. The BOR was dependent on the rotation rate and the number of electrons of 0.5 was determined from the Levich plot (*inset* of Fig. 6) at 0.1 V. Although the carbon indeed contributes to BOR, its influence is small compared to the Au/C. Concerning the BOR onset potential, bulk gold was also employed to probe, if any, advantages of using gold in the nanometric regime. Fig. 7 depicts positive-going voltammograms for Au/C, bulk Au and Vulcan carbon in deaerated 1.0 mol L^{-1} NaOH + 1.0 mmol L^{-1} $NaBH_4$ under stagnant conditions (no rotation applied). One can observe a flowing current already at −0.81 V for Au/C, which is about 200 mV more negative than those both of bulk Au (about −0.63 V) and Vulcan carbon (at around −0.58 V). Similar results were observed by Pei et al. [9] with a citrate-protected 20% Au/C catalyst generated through borohydride reduction. The authors compared the activities of carbon-supported gold nanoparticles with an Au foil towards BOR and found that the carbon-supported gold nanoparticles shifted the onset potential by 200 mV in the direction of negative potentials. Herein we were able to achieve the same potential shift with a lower-metal-content catalyst (10% Au/C) produced by a more environmentally friendly route. Although the nature of the Au particle size on carbon was polydispersive, a larger number of electrocatalytic sites might be available since no capping agent was employed for the production of the Au/C catalyst.

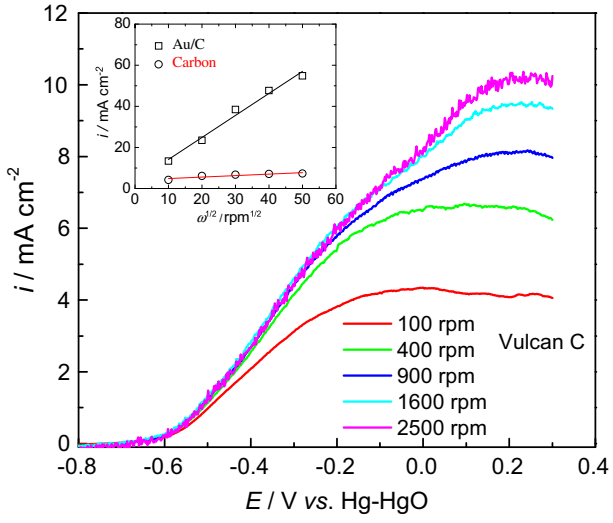

Fig. 6. Steady-state polarization curves for the BOR on pure Vulcan carbon in deaerated 1.0 mol L^{-1} NaOH + 1.0 mmol L^{-1} $NaBH_4$ at 25 °C. *Inset*: Levich plot at 0.1 V *vs.* Hg–HgO. The Levich curve for Au/C is also shown for comparison.

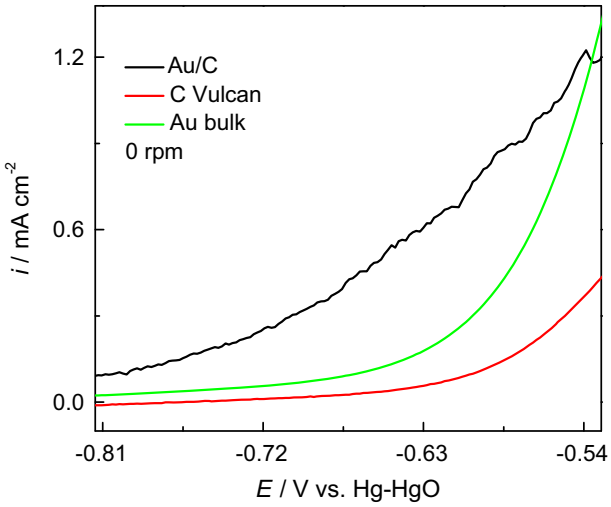

Fig. 7. Polarization curves at stagnant conditions (no rotation applied) for Au/C, bulk Au and Vulcan carbon in deaerated 1.0 mol L^{-1} NaOH + 1.0 mmol L^{-1} $NaBH_4$ at 25 °C.

4. Conclusions

Colloidal and carbon-supported AuNps were successfully generated using glycerol as reducing chemical in alkaline conditions. A maximum in the UV–vis spectrum at 520 nm was observed for different glycerol concentrations, which suggests that the average size of the AuNps is independent of the glycerol concentration in the range of 0.66 mmol L^{-1} and 3.0 mol L^{-1}. AuNps directly produced onto carbon (Au/C) were capable of oxidizing the borohydride exchanging 7.2 electrons per BH_4^-, which is close to the theoretical value of 8e$^-$. The carbon support has also an influence on the process since it exchanges 0.5 e$^-$ per BH_4^-. Finally, the gold nanoparticles decreased the onset potential for BOR by 200 mV in comparison to bulk Au. In our opinion the glycerol method should be routinely employed to produce Au nanoparticles since it is simple, inexpensive, environmentally friendly and can deliver quite active Au nanoparticles for electrocatalysis purposes.

Acknowledgements

The authors thank CNPq and FAPESP for the overall support of this research.

References

[1] M.C. Daniel, D. Astruc, Chem. Rev. 104 (2004) 293–346.
[2] J. Liu, W. Chen, X. Liu, K. Zhou, Y. Li, Nano Res. 1 (2008) 46–55.
[3] E. Roduner, Chem. Soc. Rev. 35 (2006) 583–592.
[4] S.H. Joo, S.J. Choi, I. Oh, J. Kwak, Z. Liu, O. Terasaki, R. Ryoo, Nature 412 (2001) 169–172.
[5] A.S. Arico, P. Bruce, B. Scrosati, J.M. Tarascon, W. Van Schalkwijk, Nat. Mater. 4 (2005) 366–377.
[6] S.C. Amendola, S.L. Sharp-Goldman, M.S. Janjua, M.T. Kelly, P.J. Petillo, M. Binder, J. Power Sources 85 (2000) 186–189.
[7] S.U. Jeong, R.K. Kim, E.A. Cho, H.J. Kim, S.W. Nam, I.H. Oh, S.A. Hong, S.H. Kim, J. Power Sources 144 (2005) 129–134.
[8] Z.P. Li, B.H. Liu, K. Arai, K. Asaba, S. Suda, J. Power Sources 126 (2004) 28–33.
[9] F. Pei, Y. Wang, X. Wang, P.Y. He, L. Liu, Y. Xu, H. Wang, Fuel Cells 11 (2011) 595–602.
[10] M. Chatenet, F.H.B. Lima, E.A. Ticianelli, J. Electrochem. Soc. 157 (2010) B697–B704.
[11] M.H. Atwan, C.L.B. Macdonald, D.O. Northwood, E.L. Gyenge, J. Power Sources 158 (2006) 36–44.

[12] S.C. Amendola, P. Onnerud, M.T. Kelly, P.J. Petillo, S.L. Sharp-Goldman, M. Binder, J. Power Sources 84 (1999) 130–133.
[13] M. Chatenet, F. Micoud, I. Roche, E. Chainet, J. Vondrák, Electrochim. Acta 51 (2006) 5452–5458.
[14] J.I. Martins, M.C. Nunes, R. Koch, L. Martins, M. Bazzaoui, Electrochim. Acta 52 (2007) 6443–6449.
[15] G. Rostamikia, M.J. Janik, Energy Environ. Sci. 3 (2010) 1262–1274.
[16] F.H.B. Lima, A.M. Pasqualeti, M.B. Molina Concha, M. Chatenet, E.A. Ticianelli, Electrochim. Acta, doi:10.1016/j.electacta.2012.05.030, in press.
[17] Y.G. Sun, B. Mayers, T. Herricks, Y.N. Xia, Nano Lett. 3 (2003) 955–960.
[18] B. Wiley, T. Herricks, Y.G. Sun, Y.N. Xia, Nano Lett. 4 (2004) 1733–1739.
[19] T. Herricks, J.Y. Chen, Y.N. Xia, Nano Lett. 4 (2004) 2367–2371.
[20] M. Tsuji, M. Hashimoto, Y. Nishizawa, M. Kubokawa, T. Tsuji, Chem. Eur. J. 11 (2005) 440–452.
[21] R. Harpeness, A. Gedanken, Langmuir 20 (2004) 3431–3434.
[22] M. Tsuji, M. Hashimoto, Y. Nishizawa, T. Tsuji, Chem. Lett. 32 (2003) 1114–1115.
[23] M.S. Raghuveer, S. Agrawal, N. Bishop, G. Ramanath, Chem. Mater. 18 (2006) 1390–1393.
[24] G. Glaspell, L. Fuoco, M.S. El-Shall, J. Phys. Chem. B 109 (2005) 17350–17355.
[25] X. Zhang, K.Y. Chan, Chem. Mater. 15 (2003) 451–459.
[26] D.H. Chen, S.H. Wu, Chem. Mater. 12 (2000) 1354–1360.
[27] H.H. Huang, F.Q. Yan, Y.M. Kek, C.H. Chew, G.Q. Xu, W. Ji, P.S. Oh, S.H. Tang, Langmuir 13 (1997) 172–175.
[28] U.B. Demirci, J. Power Sources 169 (2007) 239–246.
[29] A.R. West, in: Solid State Chemistry and Its Applications, John Wiley & Sons, New York, 1984.
[30] A.N. Grace, K. Pandian, Colloid. Surf. A Physicochem. Eng. Aspects 290 (2006) 138–142.
[31] F. Wu, Q. Yang, Nano Res. 4 (2011) 861–869.
[32] S. Link, M.A. El-Sayed, J. Phys. Chem. B 103 (1999) 4212–4217.
[33] A.C. Templeton, J.J. Pietron, R.W. Murray, P. Mulvaney, J. Phys. Chem. B 104 (1999) 564–570.
[34] M. Chatenet, F. Micoud, I. Roche, E. Chainet, Electrochim. Acta 51 (2006) 5459–5467.
[35] E. Gyenge, Electrochim. Acta 49 (2004) 965–978.
[36] B. Molina-Concha, M. Chatenet, Electrochim. Acta 54 (2009) 6129.
[37] M.V. Mirkin, H. Yang, A.J. Bard, J. Electrochem. Soc. 139 (1992) 2212–2217.
[38] H. Dong, R. Feng, X. Ai, Y. Cao, H. Yang, C. Cha, J. Phys. Chem. B 109 (2005) 10896–10901.
[39] M.r. Simões, S.v. Baranton, C. Coutanceau, J. Phys. Chem. C 113 (2009) 13369–13376.
[40] D.A. Finkelstein, N.D. Mota, J.L. Cohen, H.D. Abruña, J. Phys. Chem. C 113 (2009) 19700–19712.